Materials Science Forum
ISSN: 1662-9752, Vol. 924, pp 192-195
doi:10.4028/www.scientific.net/MSF.924.192

Submitted: 2017-08-21
Revised: 2017-11-14
Accepted: 2017-11-18
Online: 2018-06-05

Modeling and Simulation of Electrical Activation of Acceptor-Type Dopants in Silicon Carbide

Vito Šimonka[1,a*], Andreas Hössinger[2,b], Josef Weinbub[1,c] and Siegfried Selberherr[3,d]

[1]Christian Doppler Laboratory for High Performance TCAD, Institute for Microelectronics, TU Wien, Gußhausstraße 27-29/E360, 1040 Wien, Austria

[2]Silvaco Europe Ltd., Compass Point, St Ives, Cambridge, PE27 5JL, United Kingdom

[3]Institute for Microelectronics, TU Wien, Gußhausstraße 27-29/E360, 1040 Wien, Austria

[a]simonka@iue.tuwien.ac.at, [b]andreas.hoessinger@silvaco.com, [c]weinbub@iue.tuwien.ac.at, [d]selberherr@iue.tuwien.ac.at

Keywords: modeling, activation, silicon carbide, implantation, aluminium, boron, simulation

Abstract. We propose an empirical model to predict electrical activation ratios of aluminium- and boron-implanted silicon carbide with respect to various annealing temperatures. The obtained parameters and model extensions are implemented into Silvaco's Victory Process simulator to enable accurate predictions of post-implantation process steps. The thus augmented simulator is used for numerous simulations to evaluate the activation behavior of p-type dopants as well as for the full process simulation of a pn-junction SiC diode to extract the carrier and acceptor depth profiles and compare the results with experimental findings.

Introduction

The most common p-type doping species for silicon carbide (SiC) are aluminium (Al) and boron (B), which are typically introduced into the crystal structure via ion implantation [1]. In order to increase the electrical activation of the implanted species, it is essential to perform thermal annealing as a post-implantation step. However, modeling the effects of the thermal treatment on the implanted species in SiC is currently completely missing and the applicability of technology computer aided design (TCAD) is therefore limited. We investigate the post-implantation annealing steps of Al- and B-implanted SiC and propose an empirical model to predict the electrical activation of SiC impurities with respect to the annealing temperature.

Method

We have investigated several measurements [2–5] of the free carrier concentration as a function of sample temperature for various annealing temperatures T_A, shown in Fig. 1. The data sets have been extracted using WebPlotDigitizer [6]. Individual experimental setups with identical SiC polytypes, crystal orientations, annealing ambient, and implantation techniques have been selected. Selection of the data is necessary to ensure a focused investigation of the annealing temperature effects only. We have fitted the data with the charge neutrality equation [7] to obtain acceptor concentrations (N_A) using the ionization energy and concentration of compensated ions from [2–5], thus reproducing the fits. For a corresponding T_A the electrical activation ratios R_{act} have been calculated according to the total implanted concentration (C_{tot}) as $R_{act} = N_A / C_{tot}$. Activation ratios as a function of annealing temperature for Al- and B-implanted SiC are shown in Fig. 2. The closed and the open symbols represent results from Fig. 1 and references [8–10], respectively. A high activation (above 95 %) is achieved for $T_A > 1800$°C for Al and $T_A > 1700$°C for B impurities and a very low activation (below 10 %) is detected for $T_A < 1500$°C for both Al and B implantations. This implies that the thermal activation mechanism takes place within the temperature range 1500°C < T_A < 1800°C and must be therefore appropriately characterized. Therefore, we introduce an empirical model for electrical activation ratios of Al- and B-implanted (p-type) SiC after post-

implantation steps. The activation ratio model is inherited from our previous study of phosphorus (P) and nitrogen (N) implanted (n-type) SiC [11]. The model characterizes R_{act} as a function of T_A and assumes that the activation mechanism is instantaneous, represented by the time-independent equation

$$R_{act} = (R_{min} + R_{max})/2 + (R_{max} - (R_{min} + R_{max})/2) \tanh (k (T_A - T_{ip})), \quad (1)$$

where R_{min} and R_{max} are the minimal and maximal electrical activation ratios, respectively, k is the slope of the step, and T_{ip} the temperature at inflection of the curve.

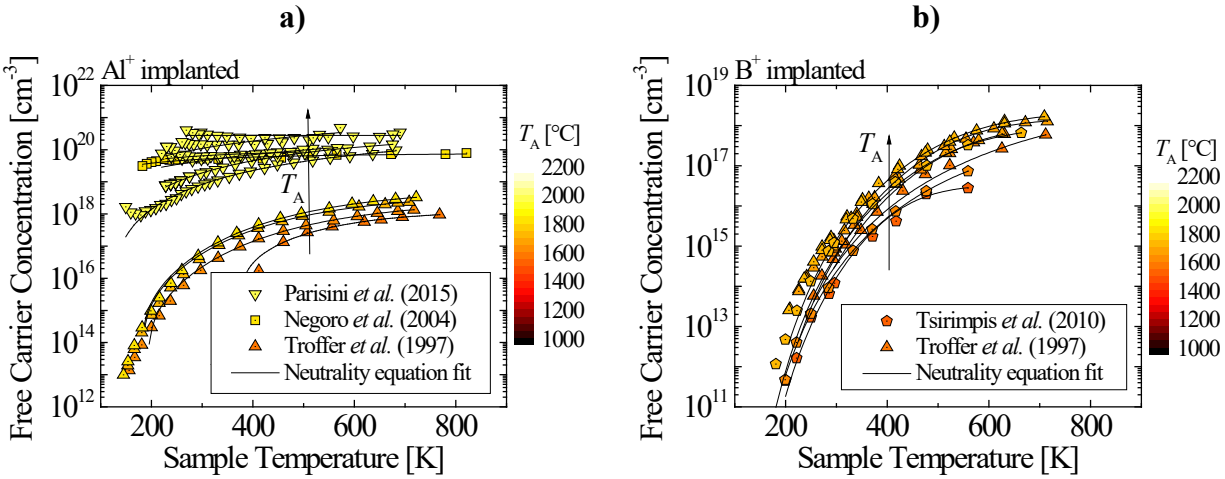

Fig. 1. Free carrier concentration as a function of sample temperature for **a)** Al- and **b)** B-implanted SiC. The symbols represent measurements [2–5], the solid lines refer to the neutrality equation fits, and the colors represent various annealing temperatures, which are explicitly seen in Fig. 2.

Results and Discussion

The data in Fig. 2 was fitted with the activation ratio model (Eq. 1), shown with solid lines. We have performed several iterations of least squares fitting [12] to minimize the numerical error. The model parameters are R_{min}=0.021, R_{max}=1.0, T_{ip}=1570°C, and k=0.015 for Al- and R_{min}=0.026, R_{max}=1.0, T_{ip}=1640°C, and k=0.011 for B-implanted SiC. The minimal activation ratio for both p-type dopants is approximately 2%, which is two-times lower compared to N- and three-times lower compared to P-implanted SiC [11]. The maximal ratio of both dopants is in this case 100% (i.e., R_{max}=1.0) for T_A>1750°C, provided that the annealing step reaches a steady state in a thermal equilibrium. The T_{ip}, i.e., the annealing temperature at which 50% activation is achieved, is highest for the B- and clearly lower for the Al-implanted SiC. Comparing the T_{ip} of the p-type dopants (this study) to the n-type dopants [11] it is evident that the latter achieve half-full activation at lower temperatures. The slope of the curve is larger for Al- and lower for B-implanted SiC, which indicates that the activation response of Al ions is closer to a step-like function. The proposed relation has been implemented into Silvaco's Victory Process simulator [13], together with the model parameters for the Al and B dopants, to evaluate the gathered findings in the context of full process simulations. Additionally, another set of parameters has been obtained by fitting the semi-empirical model from [13] to N_A (obtained in Fig. 1) as a function of C_{tot} [14]. Based on our approach we are able to predict the activation of the implants in SiC for various concentrations and annealing temperatures. We have performed numerous (i.e. 10^6) simulations to evaluate activation ratios of Al- and B-implanted SiC according to the proposed empirical relation (T_A-dependent) and semi-empirical model (C_{tot}-dependent). Fig. 3 shows phase diagrams of electrical activation regions and indicates various differences between the Al and B impurities. The evaluation of both dopant species is consistent with the results presented in [1, 5, 9, 10, 15] and is essential to optimize the post-implantation annealing processes. In addition, we have performed simulations of the

implantation and annealing process for a pn-junction diode, shown in Fig. 4, using the parameters and model extensions developed in this study. Comparisons of the doping profiles with experimental findings show good agreement for the implanted as well as the annealed samples. Considering time-critical simulations our model offers a highly attractive balance between accuracy and computational complexity.

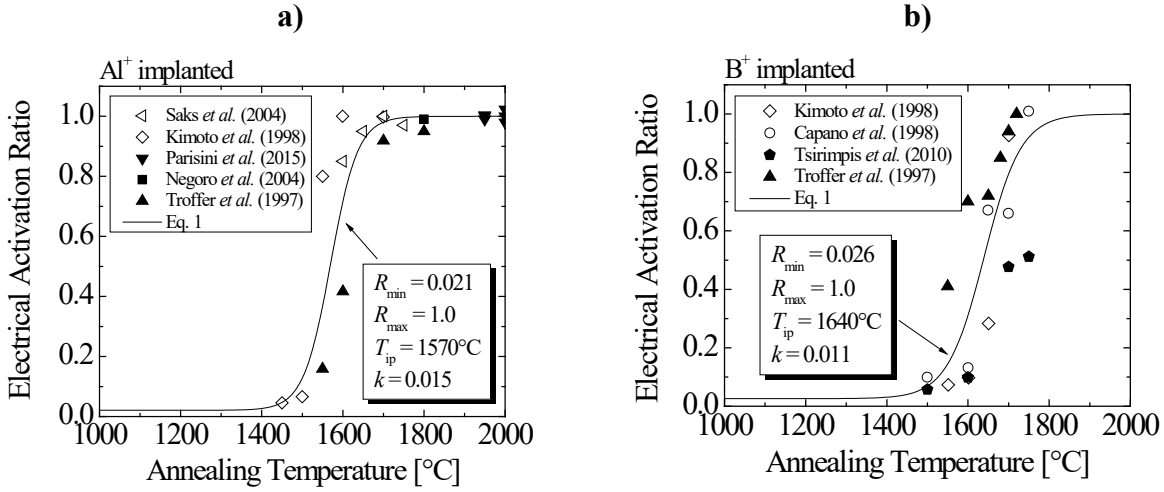

Fig. 2. Electrical activation ratio of **a)** Al- and **b)** B-implanted SiC as a function of annealing temperature. The open symbols refer to results presented in [8–10], the closed symbols are results from Fig. 1, and the solid lines show the activation ratio model fits [11].

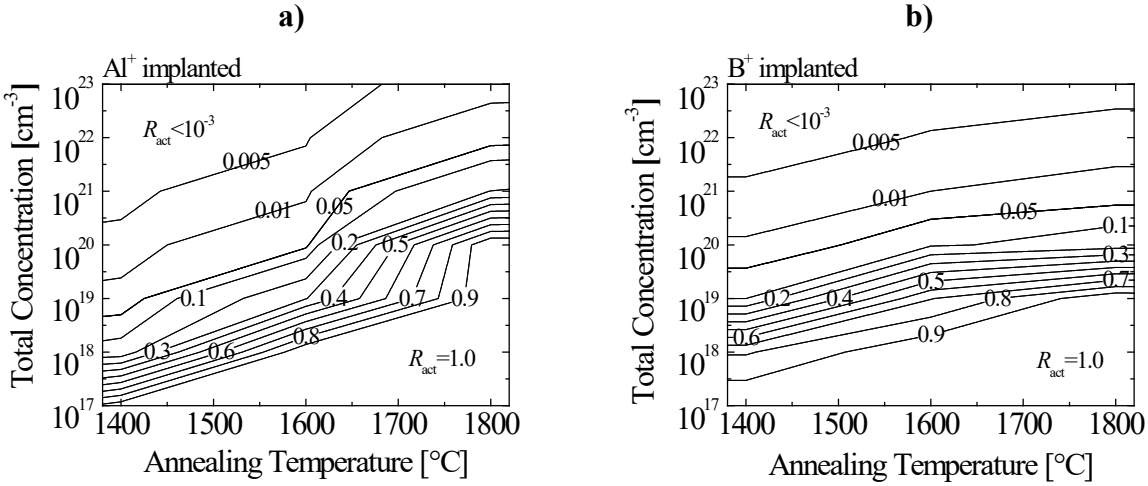

Fig. 3. Phase diagrams of predicted electrical activation ratios R_{act} for **a)** Al- and **b)** B-implanted SiC as a function of the total concentration and annealing temperature.

Summary

This study has enhanced the process simulation capabilities for SiC annealing process steps with the proposed empirical relation of the electrical activation ratios and the semi-empirical model parameters for the Al and B species in SiC. We have performed multiple simulations and obtained the model predictions of acceptor-type states in SiC after high temperature post-implantation annealing. Finally, we have compared the results with experimental data to evaluate the proposed modeling approach, which yielded a good agreement.

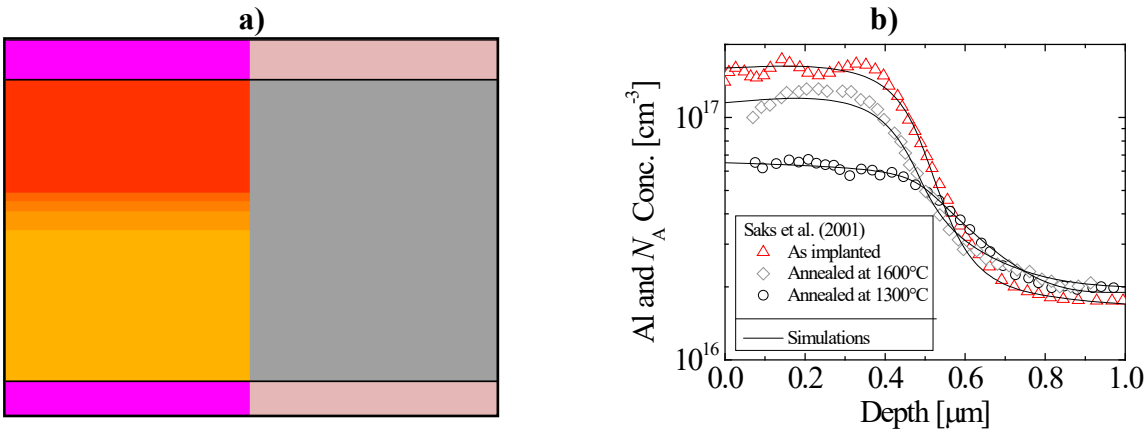

Fig. 4. **a)** Net doping (left), geometry (right), and **b)** depth profile of the pn-junction diode. Symbols refer to experimental findings from [15] and solid lines are simulations with identical variables as used in experiments.

Acknowledgements

The financial support by the Austrian Federal Ministry of Science, Research and Economy and the National Foundation for Research, Technology and Development is gratefully acknowledged.

References

[1] T. Kimoto, J. A. Cooper, Fundamentals of Silicon Carbide Technology: Growth, Characterization, Devices and Applications, John Wiley & Sons, Singapore, 2014.

[2] A. Parisini, *et al.*, J. Appl. Phys. 118 (2015) 35101-1–35101-8.

[3] Y. Negoro, *et al.*, J. Appl. Phys. 96 (2004) 4916–4922.

[4] T. Troffer et al., Phys. Status Solidi 162 (1997) 277–298.

[5] T. Tsirimpis, M. Krieger, H. B. Weber, and G. Pensl, in Proceedings of the Materials Science Forum (2010) 697–700.

[6] Information on https://automeris.io/WebPlotDigitizer/

[7] C.-M. Zetterling, Process Technology for SiC Devices, INSPEC, United Kingdom, 2002.

[8] T. Kimoto, *et al.*, J. Electron. Mater. 27 (1998) 358–364.

[9] N. S. Saks, A. V Suvorov, and D. C. Capell, Appl. Phys. Lett. 84 (2004) 5195–5197.

[10] M. A. Capano, *et al.*, J. Electron. Mater. 27 (1998) 370–376.

[11] V. Šimonka, A. Hössinger, J. Weinbub, and S. Selberherr, in Proceedings of the International Conference on Simulation of Semiconductor Processes and Devices (2017) 125-128.

[12] A. F. Hayes, Introduction to Mediation, Moderation, and Conditional Process Analysis: A Regression-Based Approach, Guilford Press, New York, 2013.

[13] Information on http://www.silvaco.com/products/tcad/

[14] V. Šimonka, *et al.*, IEEE Trans. Electron Dev. (2017), submitted.

[15] N. S. Saks, *et al.*, J. Appl. Phys. 90 (2001) 2796–2805.